Sri Lankan Journal of Physics, Vol. 18 (2017) 17-34

http://doi.org/10.4038/sljp.v18i0.8041

INSTITUTE OF PHYSICS – SRI LANKA

Research Article

Capacitive and Bioenzymevoltaic Characteristics of Photosynthetic *Chromolena Odorata* – Nanostructured Zinc Oxide System

Aanuoluwapo Raphael Obasuyi*, Aderemi Babatunde Alabi, Emmanuel Dami Kajewole, Oluwatosin Robert, Funmilayo Abejide, Toyin Joshua Adeleke and Taiye Akomolafe

Department of Physics, University of Ilorin, Ilorin, Nigeria.

Abstract

Zinc Oxide nanoparticles (ZnO) have been successfully synthesized by a chemical method at a low temperature of 60°C and dried at 80°C. The matching of the observed 2θ value with the JCPDS value of the XRD pattern showed that ZnO was synthesized. The pattern obtained showed high peaks as an indication of crystallinity at low temperature without annealing. The average grain size of the crystal obtained using Debye scherrer formular is 18.6 nm. The crystal structure lattice system is hexagonal wurzite structure. The SEM images obtained showed that the material is made up of agglomerated grains resulting in nanostructured islands. The direct optical band gap was obtained using Tauc's relationship to be 2.4 eV. A bioenzymevoltaic cell was developed in form of a Dye Sensitized Solar Cell but with a photosynthetic material: Chromolaena Odorata acting as both the dye and the electrolyte. The short circuit current of 1.5 μA and open circuit voltage of 170 mV were obtained for the continuous and residual energy on the system. We found that the device exhibited a bio-capacitive effect, as the photosynthetic material generates electron and the energy is being stored in the system as much as 39 μA with a corresponding voltage of 196 mV.

Keywords: Bioenzymevoltaics, Nanostructured, *Chromolaena Odorata*, Regeneration, Biocapacitive.

* Corresponding Author Email: anu_obasuyi@yahoo.com

http://orcid.org/0000-0001-7780-9367

1. INTRODUCTION

Renewable source of energy has attracted much attention from researchers throughout the world because of rapid diminishing in fossil fuel. Consequently, there is need for alternative source of energy. There is also climate change due to alteration in natural carbon cycle and increase in carbon dioxide in the atmosphere due to human activities that emits carbon dioxide through combustion of fossil fuels (coal, natural gas and oil) for energy, transportation and industrial use. This heat trapping gases leads to global warming. There is therefore need for a clean energy generation from sources such as solar energy, wind energy and biomass fuel.[1] Dye Sensitized Solar Cell (DSSC) is one of the attractive and cheap devices for the conversion of solar light into electrical energy since Gratzel and O'Regan firstly reported the prototype of this solar cell in 1991.[2]

Transition metal coordination compounds (ruthenium polypyridyl complexes) are used as effective sensitizers, due to their intense charge transfer absorption in the whole visible range and highly efficient metal to ligand charge transfer. Many natural dyes have also been used as photo-sensitizers, extracted from rosella (*Hibiscus sabdariffa*), blue pea (*Clitoria ternaten*) flowers. These flowers are rich in anthocyanins which is a sensitizer.[3] Chlorine E6 is another natural photosensitizer. It can be obtained from a green plant by hydrolysis of chlorophyll obtained from Spirulina having three carboxylate groups in the molecule.[4]

The abundant pigment-protein membrane complex photosystem-I (PS-I) is at the heart of the Earth's energy cycle. It is the central molecule in the ''Z-scheme'' of photosynthesis, converting sunlight into the chemical energy of life. PS-I stabilized by surfactant peptides functions as both light-harvester and charge separator in solar cells self-assembled on nanostructured semiconductors. Equally pure PS-I can be isolated from plant or bacterial extracts by porous membrane bioseparation, an inexpensive method that can be scaled up to industrial levels by simple yet highly efficient affinity binding with protein-specific epitope tags.[5]

In addition to the photosensitizer component of the dye sensitized solar cell is an electrolyte, containing redox mediator in an organic solvent affecting dye-regeneration by providing ionic conductivity in the bulk of the solution and sets the potential barrier necessary for energy conversion.[6] The common electrolyte being used in fabricating a DSSC

is the iodide triiodide electrolyte solution which facilitate the transport of charge between the working and counter electrode (Potassium iodide mixed with iodine in water – free ethylene glycol).

In this work, we report the development of a photosynthetic *Chromolaena Odorata* - Nanostructured Zinc Oxide system similar to that of a dye sensitized solar cell. The shift from the traditional DSSC configuration is the use of the encapsulated isolated photosynthetic material as both the sensitizer and an electrolyte. The sensitizer in this case is referred to as enzyme-sensitizer in which the electron is generated biologically by enzymes and injected into the semiconductor. Enzymatic processes of dark reaction photosynthesis follow immediately after the light catalytic photosynthesis process.

The energy of the absorbed light is used to split water and release electrons as shown below

$$2H_2O + Light \rightarrow O_2 + 4H^+ + 4e^- \quad (1)$$

The electrons move through a chain of electron transport molecules to reduce $NADP^+$ (Nicotinamide adenine dinucleotide phosphate), reducing it to NADPH (Nicotinamide adenine dinucleotide phosphate Hydrogen). Thus, the overall reaction of absorption of light and electron transport stages can be summarized as

$$2H_2O + 2NADP^+ + Light \rightarrow 2H^+ + 2NADPH + O_2 \quad (2)$$

The proton generated is coupled with ADP (Adenosine diphosphate) and P_i (Inorganic Phosphate) for the synthesis of ATP (Adenosine triphosphate) as.[7]

$$ADP + P_i + H^+ \leftrightarrow ATP + H_2O \quad (3)$$

The biochemical fuel NADPH and ATP generated provides the energy and the electrons in a redox reaction for the conversion of carbon dioxide to carbohydrate, illustrated in equation below:

$$3CO_2 + 9ATP + 6NADPH + Water \rightarrow glyceraldehyde3-phosphate + 8P_i + 9ADP + 6NADP^+ \quad (4)$$

The reactions that generated ATP and NADPH are called the *light reactions* of photosynthesis. The reactions that follows is *indirectly* dependent on light energy referred to as the *dark reactions* of photosynthesis because they can occur in the dark, utilizing the supplies of ATP and NADPH generated by light energy and catalyzed by the enzyme called *ribulose 1,5-bisphosphate carboxylase*.[8]

The carbon fixation is therefore powered by energy released during redox reaction by ATP and by the reducing agent NADPH which are biochemical fuel present in the prepared photosynthetic material. The continuous energy release by the encapsulated material is therefore responsible for the charge regeneration process in the system. The carbohydrate formed undergoes oxidative degradation through the process of anaerobic metabolism, which also involves the flow of electrons.

The photosynthetic material serves as our redox electrolyte due to its capacitive feature of storing the continuously biologically self-generated electrons. This characteristic is preserved by method of encapsulation of *Chromolaena Odorata* because of the tendency of degradation of the material, by this, enzymatic process is temporarily sustained. This system can therefore generate energy even in the dark, since its taking advantage of the dark reaction photosynthesis, which was initiated by solar energy.

We also report the successful synthesis of Zinc oxide nanoparticles at a low temperature of 60^0C. With peaks corresponding to hexagonal structure of zinc oxide. This suggests that zinc oxide can be prepared on non-conventional substrate such as plastic, at that temperature.

2. EXPERIMENTAL SETUP

The materials used for the formation of the *Chromolena Odorata* – Nanostructured Zinc Oxide System includes Zinc Acetate Dihydrate, isolated photosynthetic material from *Chromolena Odorata* leaves, Fluorine-doped Tin Oxide coated glass, Ammonium Hydroxide, Sodium Hydroxide, Copper Plate Electrodes and Distilled water. Characterization of the synthesized material and the system were carried out using X-ray diffractometer, UV spectrophotometer and scanning electron microscope. A magnetic stirrer with electric heater were also used to stir the sample, heat and dry the sample.

2.1 Experimental Procedure for Synthesizing ZnO nanoparticles at low temperature

The precursor was prepared by adding 25 ml of distilled water to 0.65 g of Zinc Acetate Dihydrate [$Zn(CH_3COO)_2.2H_2O$] at room temperature and 1.83 ml of Ammonium Hydroxide was then added with continuous stirring for 15 minutes to get a homogeneous solution. Thereafter, 11.65 ml of Sodium Hydroxide was added to the homogenous solution and it was stirred for 1 hour at room temperature.[9] The overall solution was heated at 60^0C for 3 hours in an oven, thereafter; it was filtered and dried at 80^0C for 5 hours in a furnace.

For a third-generation solar cells namely Dye-Sensitized Solar Cells (DSSCs), Zinc oxide (ZnO) has been widely studied as a promising alternative photoanode material. Since the inception of research on TiO_2-based DSSCs, ZnO has also been studied, since TiO_2 and ZnO have similar electron affinities and almost the same band gap energies, 3.2 and 3.3 eV respectively. ZnO, however, has much higher electron diffusivity than TiO_2.[10, 11]

2.2 Characterization Technique

2.2.1 X-Ray Diffraction (XRD)

XRD is the conventional method for exploration of crystalline structure of nanomaterials. Crystalline phase and details of the working electrode semiconductor film lattice structure are determined by XRD. XRD spectrum presents intensity versus 2θ (angle of X-ray to the sample). In the X-ray diffraction, an incident beam of X-ray is scattered from the surface and diffraction pattern is formed as a consequence of the scattering of short wavelength X-ray photons by electronic cloud of highly ordered positive ion centers within the material. Regularity and ordering of the ions forming a lattice in the sample can be detected as well.[16]

The Bragg formula $d\sin\theta = n\lambda$ is used for determination of lattice spacing in which d is the distance between special crystal planes, θ is the angle of the X-ray beam to the sample, n is an integer number and λ is the wavelength of X- ray beam. Peak broadening can be related to small crystal size, which analysed using the Scherrer formulae, $\tau = K\lambda/ \beta\cos\theta$, in which θ is considered for a specific XRD spectra peak, K is dimensionless shape factor close to 1, β is full width at half maximum of the peak and τ is the mean crystallite size for the

specific crystal plane of the peak.

2.2.2 Scanning Electron Microscope

Scattering of high energy electron beams from the surface of nanomaterials is the concept of scanning electron microscopy (SEM) to study the surface morphology of nanostructures.[17] SEM is the conventional and standard method for microscopy studies of nanostructure film morphologies such as DSSC working and counter electrodes.[18, 19]

Thicknesses of the layers in a DSSC can be measured by the cross sectional SEM which is the standard method to estimate the thickness of solid state device layers.[20] In solid state devices the thickness of every layer such as the TiO_2 porous film, the blocking layer, the metal back contact and the hole conductor capping layer directly affect the photovoltaic performance. Dependence of open-circuit voltage (V_{oc}) and hole conductivity of DSSC on the thickness of TiO_2 film was investigated by Snaith *et al*.[21, 22] Both V_{oc} and hole conductivity are reduced by increasing the TiO_2 film thickness while the dye loading increases. Therefore high extinction coefficient dyes are employed in the record efficiency DSSCs.[23]

2.2.3 UV-Vis absorption spectroscopy

Steady-state absorption spectroscopy of dye-sensitized solar cells can be used to determine the band gap of the different materials, the light harvesting efficiency of the solar cell, material's concentrations within the device and the extinction coefficients of dyes. The absorbance of a sample ($A(\lambda)$) as a function of the wavelength (λ) is defined by the logarithmic ratio of the incoming light intensity ($I_0(\lambda)$) and the transmitted light intensity ($I_t(\lambda)$) through a sample. Absorption spectra are therefore usually obtained by measuring the light transmitted through the sample and the light transmitted through a non- absorbing reference in the same set-up. The extinction coefficients ($\epsilon(\lambda)$) or concentrations of dyes in solution (C) can be estimated using the Beer-Lambert law: $A(\lambda)=\epsilon(\lambda)Cl$, where l is the optical length of the used cuvette (usually 1 cm). For accurate determinations of the extinction coefficient, C should be rather low to prevent light scattering and aggregation in the solution. Furthermore, it should be noted that the error in the measurement becomes very large at high absorbance values when the intensity of transmitted light becomes very small. When measuring solid samples, the absorption coefficient α, tends to be used instead of the

extinction coefficient. The bandgap energies of semiconductors (E_g) can be determined from measurements of the absorption coefficient. For direct bandgap semiconductors, the absorption coefficient is related to the photon energy ($E_p h$) near the absorption edge by: $\alpha \propto \sqrt{(E_p h - E_g)}$. For indirect bandgap semiconductors this relation is: $\alpha \propto (E_p h - E_g)^{2}$.[24]

2.3 Preparation of *Chromolaena Odorata*

The leaves of the plant was plucked at Ilorin, Nigeria, with geographic coordinates of 8°30′N 4°33′E. The leaf is locally known as "*Ewe-Akintola"*, it is greenish in color and soft in texture. A good quantity was cut into pieces without adding water and then crushed and ground into a green paste.

It is a photosynthetic material which converts solar radiation to chemical energy and this chemical energy is more functional in DSSC. This is achieved by fixing carbon dioxide from the atmosphere. Because of the conversion of carbon dioxide to metabolites, such as starches, sugars and carbohydrates, oxygen is produced as a by-product.[12] The material is abundantly available in the western part of Africa.

2.4 Fabrication of the Bioenzymevoltaic System

The system was fabricated as shown in Figure 1. The Fluorine-doped Tin Oxide coated glass was used as the anode of the system upon which an open ended encapsulator was attached and the low temperature synthesized Zinc Oxide nanostructures in microscale was attached to the surface of the Fluorine-doped Tin Oxide.

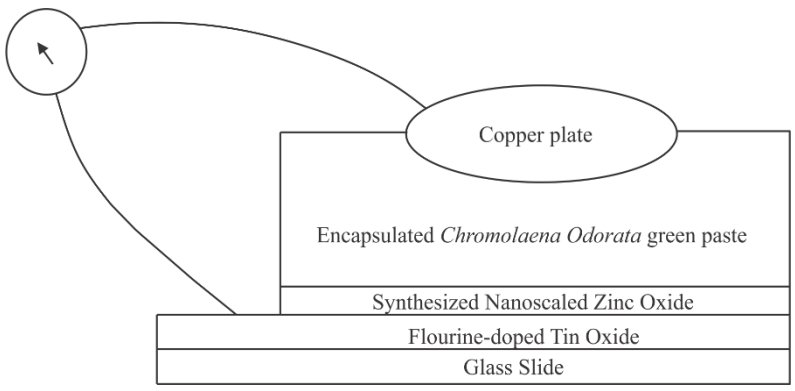

Figure 1: Configuration of the Chromolaena Odorata – Zinc Oxide system

The photosynthetic enzymatic material acting as the dye and an electrolyte was then attached to the Zinc Oxide inside the encapsulator and a copper plate was used as the back contact. The device is of 10cm in height and of 5cm wide.

3. RESULTS AND DISCUSSION

3.1 Structural Characterization

3.1.1 X-ray Diffractometer (XRD) Analysis

The structural properties of the Zinc Oxide prepared at low temperature 60^0C was characterized with X-ray diffractometer with 2θ values range between 20-80^o. Figure 2 shows the XRD pattern for the ZnO nanostructured particles.

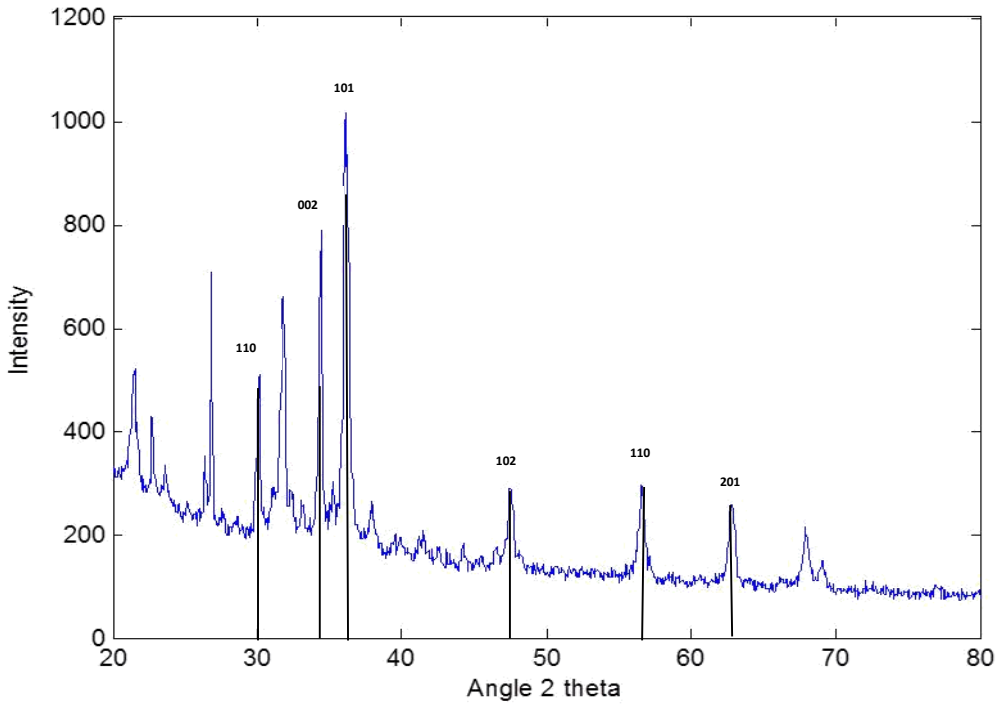

Figure 2: XRD pattern of ZnO nanoparticles synthesized at a low temperature

Diffraction peaks in the pattern obtained are easily indexed to the Zinc Oxide hexagonal crystal structure and are in good agreement with the database 2θ values of ZnO

with lattice constant plane oriented in the direction (101). Data obtained at each peak was used to calculate the grain size as shown in Table 1 for ZnO.

Table 1: Grain Size of ZnO at Peak values

2θ JCPDS card	2θ Observed	β (FWHM)	Grain Size(nm)	Crystal Plane Orientation
31.7702	31.78	0.434	19.1	110
34.4220	34.42	0.433	20.1	002
36.2531	36.29	0.434	20.1	101
47.5390	47.61	0.570	14.6	102
56.6032	56.62	0.475	17.5	110
67.6930	67.80	0.570	17.5	201

The crystallite size D was estimated from the peak width with Scherrer's formula equation

$$g = \frac{0.94\lambda}{\beta cos\theta}, \tag{5}$$

where λ is the X-ray wavelength (0.1541nm), β is the full width at half maximum (FWHM) of a diffraction peak, θ is the diffraction angle, and *K* is the Scherrer's constant. [13]

According to the diffraction peak positions and the width at half-maximum, the mean size of ZnO can be estimated to be approximately 18.2 nm. This confirms that the material (ZnO) synthesized is nanostructured scaled material.

The nanocrystalline Zinc Oxide was successfully synthesized at a low temperature 60°C. The route of preparation is a unique and of great advantage because there is no need for annealing the as-prepared material at high temperature before achieving a crystal structure as illustrated in the XRD pattern shown above.

3.1.2 Scanning Electron Microscope (SEM) analysis

Scanning electron microscopy is a convenient technique to study the microstructure of ZnO nanoparticle samples. This was employed to characterize the surface morphology. Unlike bulk materials, properties of nanomaterials are strongly correlated to shape. This shape is attained during growth through a self-assembling process dictated by the interplay of size and molecular interactions. Deviations from bulk properties become prominent as the

size of nanomaterials starts to be comparable to the size of constituent molecules or to some other characteristic length scale like electron mean-free path. In a typical application, one deals with a collection of nanomaterials, which may be dispersed in a matrix forming a composite material. Properties of this nanocomposite are controlled not only by morphology of individual nanomaterials, but also by the nature of interactions, which, in turn, is determined by the distribution of the nanomaterials in the matrix.[14]

Figure 3 shows the SEM morphology of the synthesized Nanostructured ZnO particles. It demonstrates clearly aggregation of nanoparticles in formation of islands of Zinc oxide nanoparticles because of agglomeration of grains. The occurrence of some voids of ZnO on the FTO was indicated on the SEM images and this voids are linked to the relaxation of the FTO/ZnO interface stress.

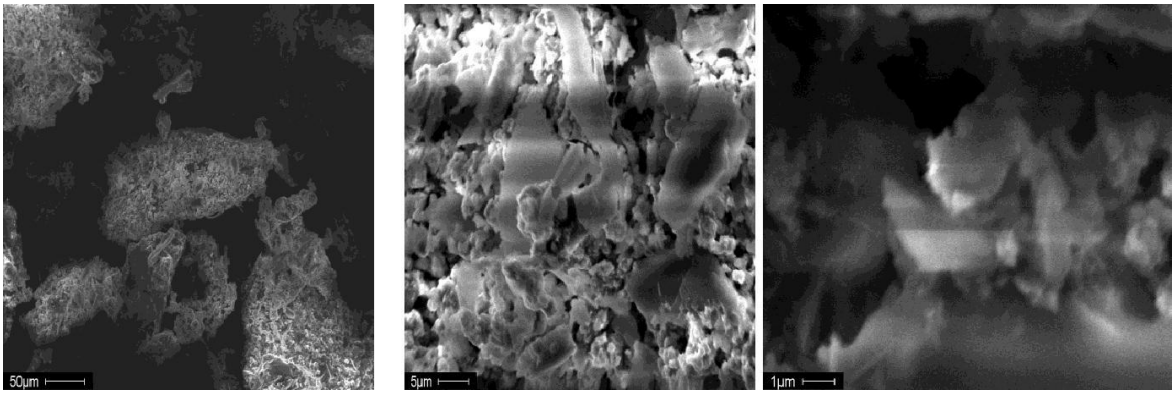

Figure 3: Low magnification SEM image of Zinc Oxide Nanostructured Particles

3.2 Optical Characterization

3.2.1 UV-Visible Spectroscopy

The absorption spectrum of synthesized zinc oxide nanoparticle is as shown in Figure 4, showing a high absorption within the visible region.

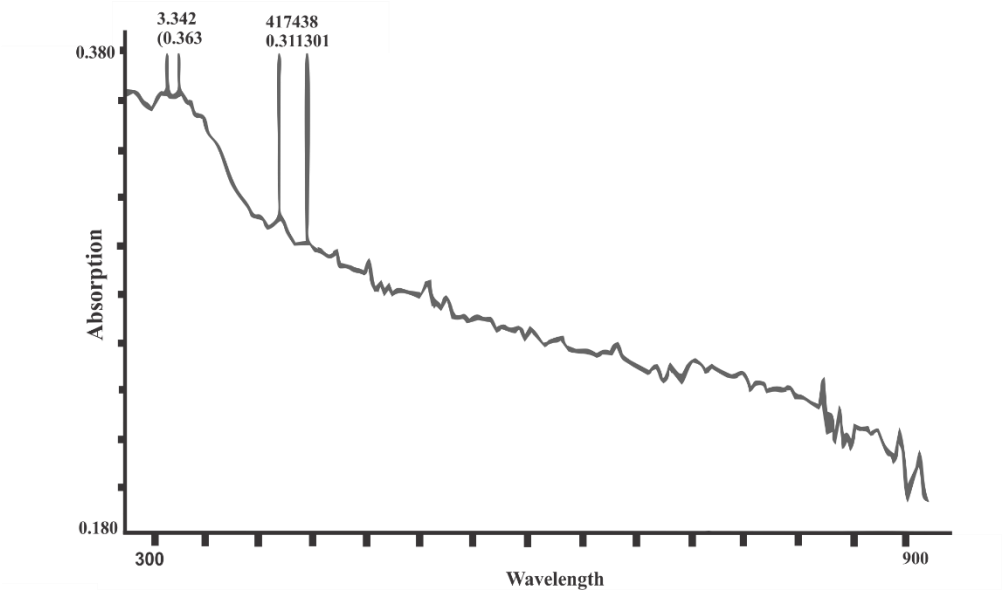

Figure 4: Absorption Spectrum of Zinc Oxide nanoparticle

It exhibits strong absorption bands at about 323, 342, 417 and 438 nm. It is also evident that significant sharp absorption of ZnO indicates the monodispersed nature of the nanoparticle distribution.

The band-gap energy (Eg) was obtained through the graph plotted with the aid of the Tauc relationship which is given below

$$(\alpha h\nu)^r = A\left(h\nu - E_g\right) \tag{6}$$

where $r = 0.5$ for the direct transition band-gap and $r = 2$ for the indirect transition band-gap.

A graph of $(\alpha h\nu)^2$ versus $h\nu$ is shown in Figure 5. By extrapolating the straight-line portion of the graph to energy axis, the band gap of the samples is obtained. The band gap is found to be2.4 eV.

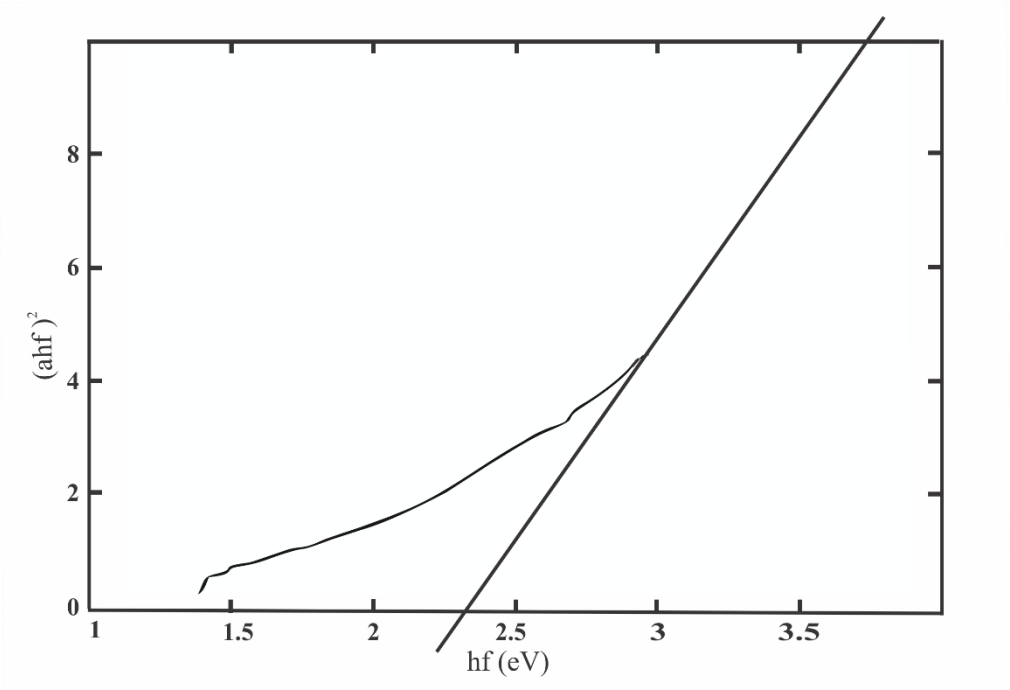

Figure 5: Band-gap determination of Zinc Oxide nanoparticles

3.3 Bio-Electrical Characterization of Photosynthetic *Chromolena Odorata* – Nanostructured Zinc Oxide System

3.3.1. Current generated with Time

The quantitative values of the current generated with time in minutes was measured and illustrated by the graph in Figure 6. The current regenerated (indicated by the arrow pointing upwards) after each discharge is observed to be increasing with time from about 8 μA after 30 minutes to about 40 μA after 390 minutes. The discharge occurs when the system is short circuited but does not reduce to zero referred to, here, as residual current, due to a continuous regeneration of charges biologically through a redox reaction, that are injected into zinc oxide.

The increasing regenerated accumulated charges in the photosynthetic material with time as shown in Figure 6, injected in the zinc oxide are stored in the system until they are discharged during measurement of the short circuit current. This illustrates the capacitive feature of the system.

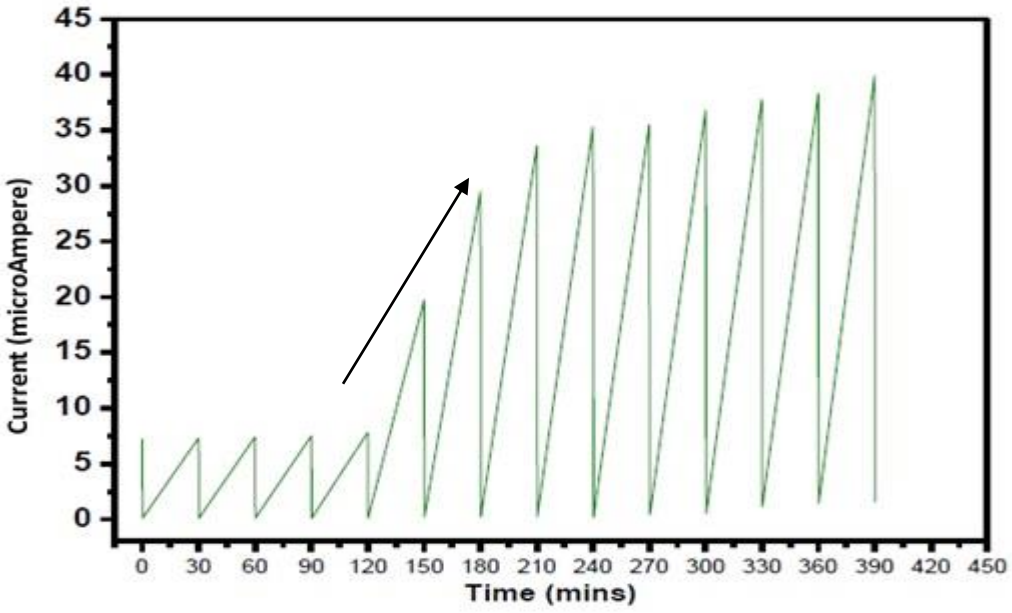

Figure 6: Current – Time graph of the System representing the discharging and charging characteristic of the system.

We know that, in a Dye Sensitized Solar Cell, after electron injection, the ground state of the dye is subsequently restored by electron donation from the electrolyte; this step is often referred to as the regeneration reaction. The electrolyte is usually an iodide/triiodide redox couple dissolved in a liquid organic solvent. The regeneration of the sensitizer by iodide intercepts the recapture of the injected electron by the oxidized dye. The iodide is in turn regenerated by the reduction of triiodide at the counter electrode, with the electrical circuit being completed via electron migration through the external load. The oxidized dye molecules are reduced by the electrons in electrolyte and, simultaneously, the electrolyte is regenerated by the electrons injected from the counter electrode.[15]

The rate of regeneration of the charges were obtained using the equation below.

$$Rate = \frac{Peak\ regenerated\ Current\ per\ period - Initial\ Residual\ Current\ for\ the\ same\ period}{Period\ of\ Current\ Regeneration}. \qquad (7)$$

Each regeneration period is represented by the time taken for the current to get to the peak of the regenerated current from the initial residual value of the current. The graph of the rate of charge regeneration with time is as shown in Figure 7.

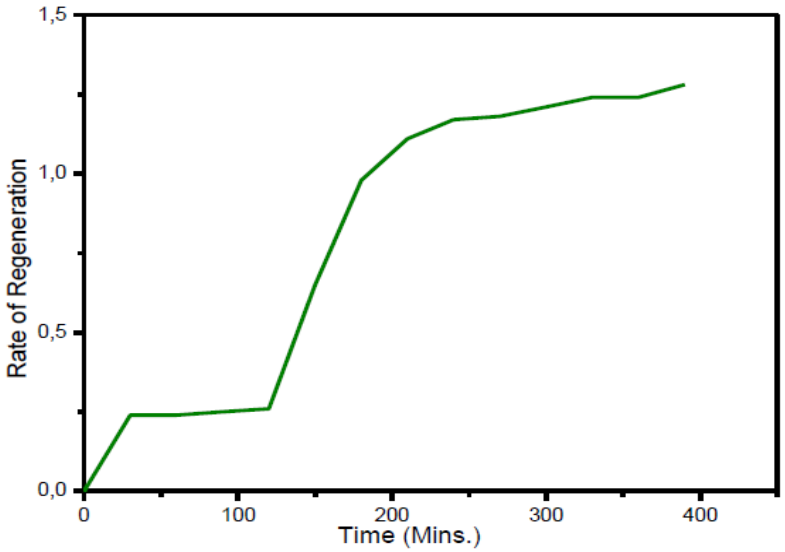

Figure 7: Rate of Charge regeneration with Time

The residual current in the system represents the value of the charges/energy stored continuously on the system per time. This is due to continuous generation of charge by biological means. The energy does not at any point in time reduce to zero as shown in figure 8. The residual current increases with time until becoming steady after 350 minutes.

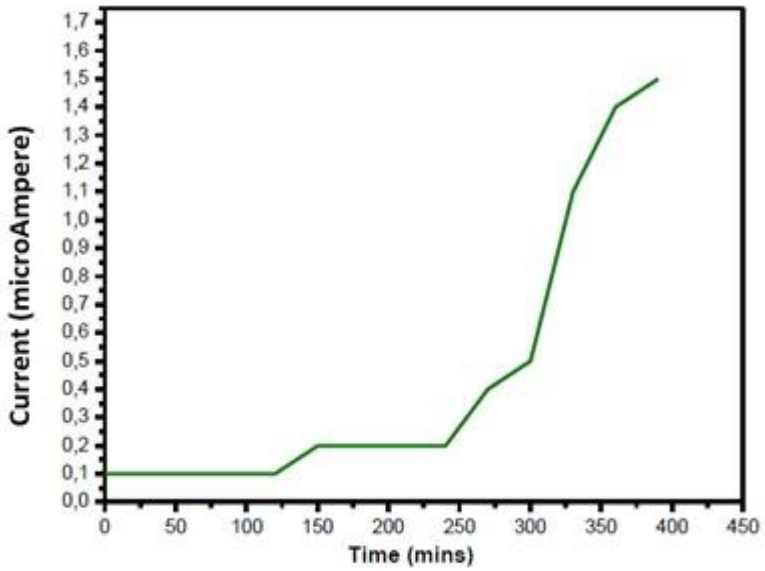

Figure 8: Residual current generation against Time

3.3.2. Current – Voltage Measurement of the System

Charge generation is through two main processes. These are Enzymatic reduction of Carbon dioxide during which chemical fuel such as ATP and $NADP^+$ which are charge carriers releases electron by redox reaction as seen in Figure 9. The other stage of charge generation is the oxidative degradation of carbohydrate as seen in Figure 10. The electrons generated are injected into the large band gap semiconductor ZnO.

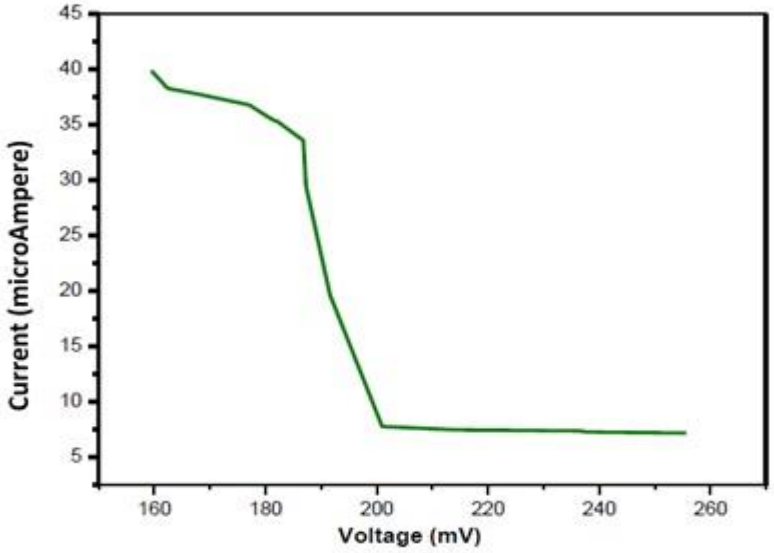

Figure 9: Current – Voltage characteristic graph of the capacitive system

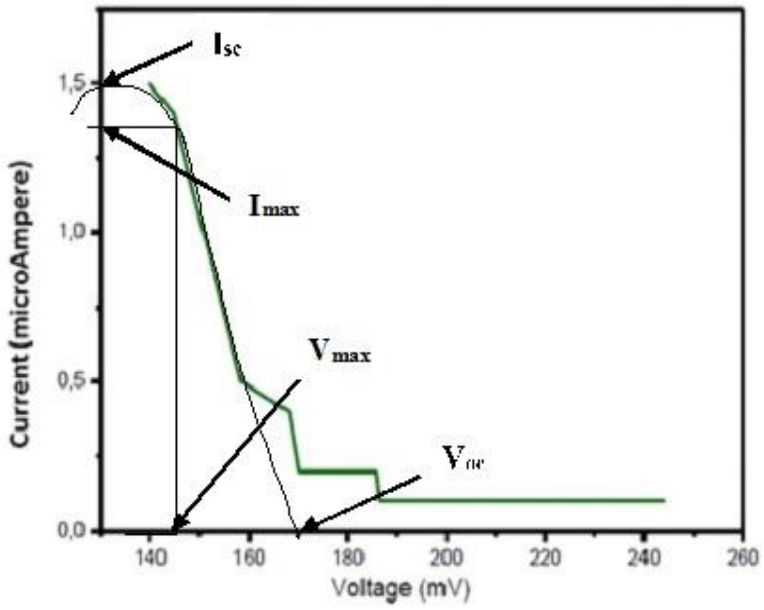

Figure 10: Current - Voltage characteristics of residual energy generated by the system

P_{max} is the product of current and voltage at maximum power point (MPP).

P_{max} = Imax X Vmax

Fill factor (FF) of the device is the ratio of P_{max} to the product of I_{sc} and V_{oc}.

$$FF = \frac{P_{max}}{I_{sc} x V_{oc}} x100$$

From Figure 10, the Isc, Voc, Imax, Vmax, FF and Pmax for the I-V characteristic of the residual energy generated are estimated to be 1.5 μA, 170 mV, 1.3 μA, 148 mV, 75.45% and 192.4 x 10^{-9}w respectively.

4. CONCLUSION

A system with charge storing capacity has been developed in the dye sensitized solar cell configuration. It exhibits a bioenzymevoltaic effect by sensitizing the large band gap zinc oxide with electron generated enzymatically. The conventional electrolyte iodide/triiodide is here replaced with encapsulated photosynthetic material with self-generated charges by the enzyme (RUBISCO) through dark reaction photosynthesis. The capacitive effect is shown by the increase in the short circuit current Isc with time. The regenerative effect is illustrated with restoration increase in the charge on the system. The large band gap sensitized nanostructured zinc oxide was synthesized using a wet chemistry at low temperature of about 60°C. The XRD pattern shows a nanocrystalline property of the material, cubic structure crystal phase. The direct optical band gap obtained is 2.4 eV. A short circuit current of 1.5 μA was obtained with a corresponding OCV of 170 mV for the bioemymevoltaic capacity of the system and highest short circuit current for the capacitive effect is 39 μA and the corresponding OCV is 196 mV.

ACKNOWLEDGEMENT

Authors gratefully acknowledge the support of Physics Department, University of Ilorin in carrying out this work. OAR appreciate CIMAV for his doctoral program.

REFERENCES

1. P. Wang, S. Zakeeruddin, J. Moser, M. Nazeeruddin, T. Sekiguchi & M. Grätzel, *A stable quasi-solid-state dye-sensitized solar cell with an amphiphilic ruthenium sensitizer and polymer gel electrolyte*. Nature Materials **2,** (2003), 402-407. DOI: http://doi.org/10.1038/nmat904

2. S. Hao, J. Wu, Y. Huang & J. Lin, *Natural dyes as photosensitizers for dye-sensitized solar cell*. Solar Energy **80,** (2006), 209-214. DOI: https://doi.org/10.1016/j.solener.2005.05.009

3. K. Wongcharee, V. Meeyoo & S. Chavadej, *Dye-sensitized solar cell using natural dyes extracted from rosella and blue pea flowers*. Solar Energy Materials and Solar Cells **91,** (2007), 566-571. DOI: https://doi.org/10.1016/j.solmat.2006.11.005

4. Y. Amao & T. Komori, *Bio-photovoltaic conversion device using chlorine-e_6 derived from chlorophyll from Spirulina adsorbed on a nanocrystalline TiO_2 film electrode.* Biosensors and Bioelectronics **19,** (2004), 843-847. DOI: https://doi.org/10.1016/j.bios.2003.08.003

5. A. Mershin, K. Matsumoto, L. Kaiser, D. Yu, M. Vaughn, Md. K. Nazeeruddin, B. D. Bruce, M. Gratzel & S. Zhang, *Self-assembled photosystem-I biophotovoltaics on nanostructured $TiO_2$and ZnO*. Scientific Reports **2,** (2012), 234. DOI: https://doi.org/10.1038/srep00234

6. J. Gong, J. Liang & K. Sumathy, *Review on dye-sensitized solar cells (DSSCs): Fundamental concepts and novel materials*. Renewable and Sustainable Energy Review **16,** (2012), 5848-5860. DOI: https://doi.org/10.1016/j.rser.2012.04.044

7. J. M. Berg, J. L. Tymoczko & L. Stryer, *A Proton Gradient Powers the Synthesis of ATP*. Biochemistry (5th Edition), W.H. Freedman, Section 18.4, 2002. Available from: http://www.ncbi.nlm.nih.gov/books/NBK22388/

8. H. Lodish, A. Berk, S.L. Zipursky, P. Matsudaira, D. Baltimore & J. Darnell, *Molecular Cell Biology* (4th Edition), W.H. Freeman (2000), New York.

9. N. Singh, R. M. Mehra, A. Kapoor & T. Soga, *ZnO based quantum dot sensitized solar cell using CdS quantum dots*. Journal of Renewable and Sustainable Energy **4,** (2012), 013110. DOI: http://dx.doi.org/10.1063/1.3683531

10. C-P. Lee, C-Y. Chou, C-Y. Chen, M-H. Yeh, L-Y. Lin, R. Vittal, C-G. Wu & K-C. Ho, *Zinc oxide-based dye-sensitized solar cells with a ruthenium dye containing an alkyl bithiophene group*. Journal of Power Sources **246,** (2014), 1-9. DOI: https://doi.org/10.1016/j.jpowsour.2013.05.101

11. S. Rani, P. Suri, P.K. Shishodia & R.M. Mehra, *Synthesis of nanocrystalline ZnO powder via sol–gel route for dye-sensitized solar cells*. Solar Energy Materials and Solar Cells **92,** (2008), 1639-1645. DOI: https://doi.org/10.1016/j.solmat.2008.07.015

12. J. C. Rooke, A. Léonard, C. F. Meunier , H. Sarmento, J-P. Descy & B-L. Su, *Hybrid photosynthetic materials derived from microalgae Cyanidium caldarium encapsulated within silica gel*. Journal of Colloid and Interface Science **344,** (2010), 348-352. DOI: https://doi.org/10.1016/j.jcis.2009.12.053

13. R.C. Singh, O. Singh, M.P. Singh & P.S. Chandi, *Synthesis of zinc oxide nanorods and nanoparticles by chemical route and their comparative study as ethanol sensors*. Sensor and Actuators B **135,** (2008), 352-357. DOI: https://doi.org/10.1016/j.snb.2008.09.004

14. M.K. Sanyal, A. Dalta & S. Hazra, *Morphology of nanostructured materials*. Pure Appl. Chem. **74,** (2002), 1553. **DOI:** https://doi.org/10.1351/pac200274091553

15. A. Omar & H. Abdullah, *Electron transport analysis in zinc oxide-based dye-sensitized solar cells: A review*. Renewable and Sustainable Energy Reviews **31,** (2014), 149-157. DOI: https://doi.org/10.1016/j.rser.2013.11.031

16. O. H. Seeck & Bridget Murphy, *X-Ray Diffraction: Modern Experimental Techniques*, Pan Stanford, 2015.

17. W. Zhou, R. P. Apkarian & Z. L. Wang, *Scanning Microscopy for Nanotechnology: Techniques and Applications*, Springer, 2007. 100.

18. S. Thomas, T. G. Deepak, G. S. Anjusree, T. A. Arun, S. V. Nair & A. S. Nair, *A review on counter electrode materials in dye-sensitized solar cells.* J. Mater. Chem. A Mater. Energy Sustain, **2,** (2014), 4474-4490. DOI: http://doi.org/10.1039/C3TA13374E

19. Q. Zhang & G. Cao, *Nanostructured photoelectrodes for dye-sensitized solar cells*. Nano Today, **6,** (2011), 91-109. DOI: https://doi.org/10.1016/j.nantod.2010.12.007

20. H. J. Snaith & L. Schmidt-Mende, *Advances in Liquid-Electrolyte and Solid-State Dye-Sensitized Solar Cells*. Adv. Mater., **19,** (2007), 3187-3200. DOI: http://doi.org/10.1002/adma.200602903

21. H. J. Snaith, L. Schmidt-Mende, M. Grätzel & M. Chiesa, *Light intensity, temperature, and thickness dependence of the open-circuit voltage in solid-state dye-sensitized solar cells*. Phys. Rev. B, **74,** (2006), 045306. DOI: https://doi.org/10.1103/PhysRevB.74.045306

22. H. J. Snaith, R. Humphry-Baker, P. Chen, I. Cesar, S. M. Zakeeruddin & M. Grätzel, *Charge collection and pore filling in solid-state dye-sensitized solar cells.* Nanotechnology, **19,** (2008), 1-12. DOI: https://doi.org/10.1088/0957-4484/19/42/424003

23. H. J. Snaith, A. J. Moule, C. Klein, K. Meerholz, R. H. Friend & M. Grätzel, *Efficiency Enhancements in Solid-State Hybrid Solar Cells via Reduced Charge Recombination and Increased Light Capture*. Nano Lett., **7,** (2007), 3372-3376. DOI: http://doi.org/10.1021/nl071656u

24. R. Memming & D. Bahnemann, *Semiconductor electrochemistry*, Wiley-V 50 C H Verlag Gmbh, New York, 2001.